Neuroscience Research 109 (2016) 28–34

Contents lists available at ScienceDirect

Neuroscience Research

journal homepage: www.elsevier.com/locate/neures

Homeostatic changes in neuronal network oscillations in response to continuous hypoperfusion in the mouse forebrain

Yuya Nishimura[a], Reimi Abe[a], Takuya Sasaki[a,*], Yuji Ikegaya[a,b,**]

[a] Graduate School of Pharmaceutical Sciences, The University of Tokyo, 7-3-1 Hongo Bunkyo-ku, Tokyo 113-0033, Japan
[b] Center for Information and Neural Networks, Suita City, Osaka 565-0871, Japan

ARTICLE INFO

Article history:
Received 28 December 2015
Received in revised form 16 February 2016
Accepted 22 February 2016
Available online 2 March 2016

Keywords:
Hypoperfusion
Hippocampus
Neocortex
Local field potential
Network

ABSTRACT

Neuronal activity is highly sensitive to changes in oxygen tension. In this study, we examined the impact of hypoxic/ischemic conditions on neuronal ensemble activity patterns in the mouse brain using in vivo extracellular electrophysiological recordings from up to 8 sites in the thalamus, dorsal hippocampus, and neocortex, while cerebral hypoperfusion was induced by unilateral carotid artery occlusion. After a few minutes, the occlusion triggered a rapid change in the power of the local field oscillations. In the hippocampus, but not in the neocortex, the absolute power changes at all frequency ranges (relative to the baseline) became less pronounced with time, and no significant changes were observed 30 min after the occlusion-induced hypoperfusion. We also tested whether continuous hypoperfusion induced by the occlusion for up to 1 week alters neuronal activity. In the hippocampus and the thalamus, the chronic occlusion did not lead to a reduction in the power of the local field oscillations. These results indicate that certain neuronal populations have the ability to maintain internal neurophysiological homeostasis against continuous hypoperfusion.

1. Introduction

Normal brain function is maintained by a stable energy supply delivered by continuous blood flow. Certain diseases that cause an insufficient blood supply to the brain, such as cardiac arrest, stroke and head trauma, can result in cerebral hypoxic/ischemic conditions, leading to long-term disability and neuronal death. Numerous studies have revealed signaling pathways and molecular mechanisms underlying the neuronal degeneration observed with hypoxia/ischemia (Eltzschig and Eckle, 2011). However, there is still a lack of information on the pathophysiological basis of ischemia.

In normal physiological states, the mammalian forebrain generates diverse rhythmic activity with a frequency band ranging from approximately 0.1 Hz to 200 Hz. This rhythmic activity is thought to link the firing of single neurons into collective neuronal ensembles and facilitate efficient information processing, including cognition, learning and memory (Buzsaki, 2006). However, only a few experimental studies have examined how decreased blood flow affects ongoing neuronal oscillations (Barth and Mody, 2011; Buzsaki et al., 1989; Monmaur et al., 1986). Unresolved questions include (1) how individual brain regions alter their network activity patterns under hypoxic/ischemic conditions and (2) how ischemia-induced activity patterns undergo further changes during post-ischemic survival periods.

To address these issues, we examined electrical activity patterns following the induction of hypoxia/ischemia using a multi-channel electrical recording system to examine the mouse thalamo-cortico-hippocampal network. The hypoxic/ischemic states were acutely or chronically induced by (i) common carotid artery occlusion (CCAO) (Ohtaki et al., 2005) and (ii) photothrombosis of blood vessels (Barth and Mody, 2011) to induce moderate global hypoperfusion and severe focal ischemia, respectively. Power spectrum analyses of local field potentials (LFPs) revealed the pathophysiological effects of hypoxia/ischemia on the temporal activity patterns of neuronal networks in different brain regions.

2. Materials and methods

2.1. Animals

All experiments were performed with the approval of the experimental animal ethics committee at the University of Tokyo

* Corresponding author. Tel.: +81 3 5841 4783; fax: +81 3 5841 4786.
** Corresponding author at: Graduate School of Pharmaceutical Sciences, The University of Tokyo, 7-3-1 Hongo Bunkyo-ku, Tokyo 113-0033, Japan. Tel.: +81 3 5841 4780; fax: +81 3 5841 4786.
E-mail addresses: tsasaki@mol.f.u-tokyo.ac.jp (T. Sasaki), yuji@ikegaya.jp (Y. Ikegaya).

http://dx.doi.org/10.1016/j.neures.2016.02.007
0168-0102/

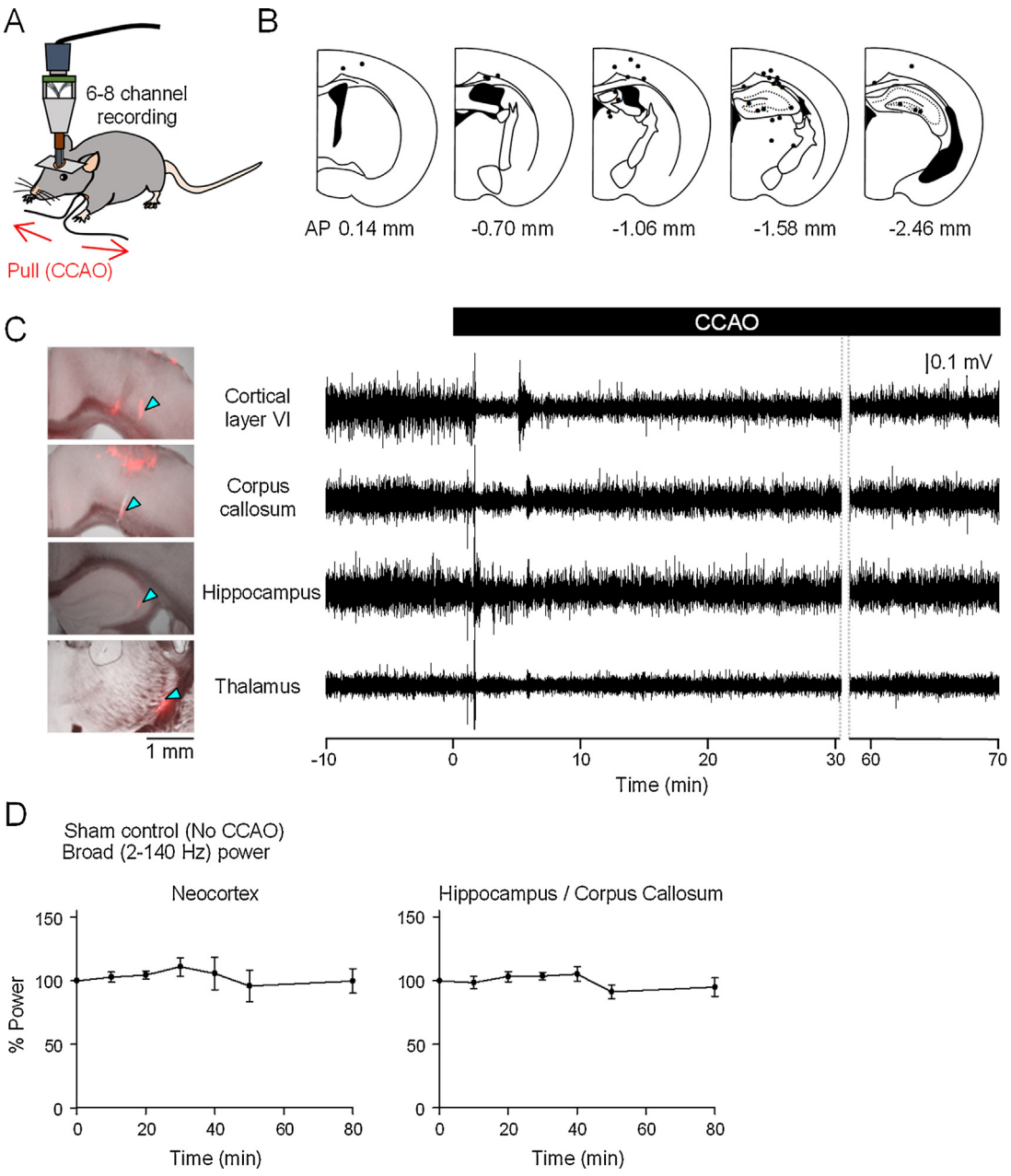

Fig. 1. Simultaneous in vivo electrophysiological recordings from the thalamo-cortico-hippocampal network during the induction of CCAO. (A) Illustration of the set-up used for multichannel recordings of neuronal activity during cerebral hypoperfusion. CCAO was produced by pulling both ends of a string looped around the common carotid artery. (B) Histological verification of the recording sites in sequential coronal brain sections. Black dots indicate the endpoints of electrode tracts from the acute CCAO experiments ($n = 7$ mice). (C) Representative simultaneous recordings of extracellular LFP signals from four brain regions from a mouse. CCAO was induced at time 0 min. The corresponding recording sites are indicated by the blue arrows in the left panels. (D) Time changes in LFP power at a broad frequency (2–140 Hz) band for 80 min in the neocortex (left, $n = 6$ recordings from 4 mice) and hippocampus/corpus callosum (right, $n = 12$ recordings from 4 mice).

(approval number: P24-70) and according to the NIH guidelines for the care and use of animals. A total of 17 male C57BL/6 mice (6–10 weeks old) with a preoperative weight of 18–28 g were used in this study. The animals were maintained on a 12-h light/dark schedule with lights off at 7:00 PM. All animals were purchased from SLC (Shizuoka, Japan). Mice were housed individually following surgery.

2.2. Surgery to induce brain hypoxia/ischemia

One of the following three surgeries was performed on each animal: acute common carotid artery occlusion (CCAO), chronic CCAO, and photothrombosis. For acute CCAO, mice were anesthetized with urethane (1.0 g/kg body weight, intraperitoneal injection). The left common carotid artery was exposed, and an elastic string with a diameter of ~1 mm was used to form a loop (~1-mm wide) surround the artery. Electrophysiological recording was then performed as described below. During recording, the loop was manually closed by pulling both ends of the string (Fig. 1A). For chronic CCAO, mice were first anesthetized with pentobarbital (0.38 g/kg bodyweight, intraperitoneal injection), and the left common carotid artery was ligated with the same type of string used for acute CCAO. The mice were allowed to recover for one week following the surgery, and electrophysiological recordings were performed as described below (Fig. 2). For induction of photothrombosis, mice were anesthetized with urethane (1.0 g/kg

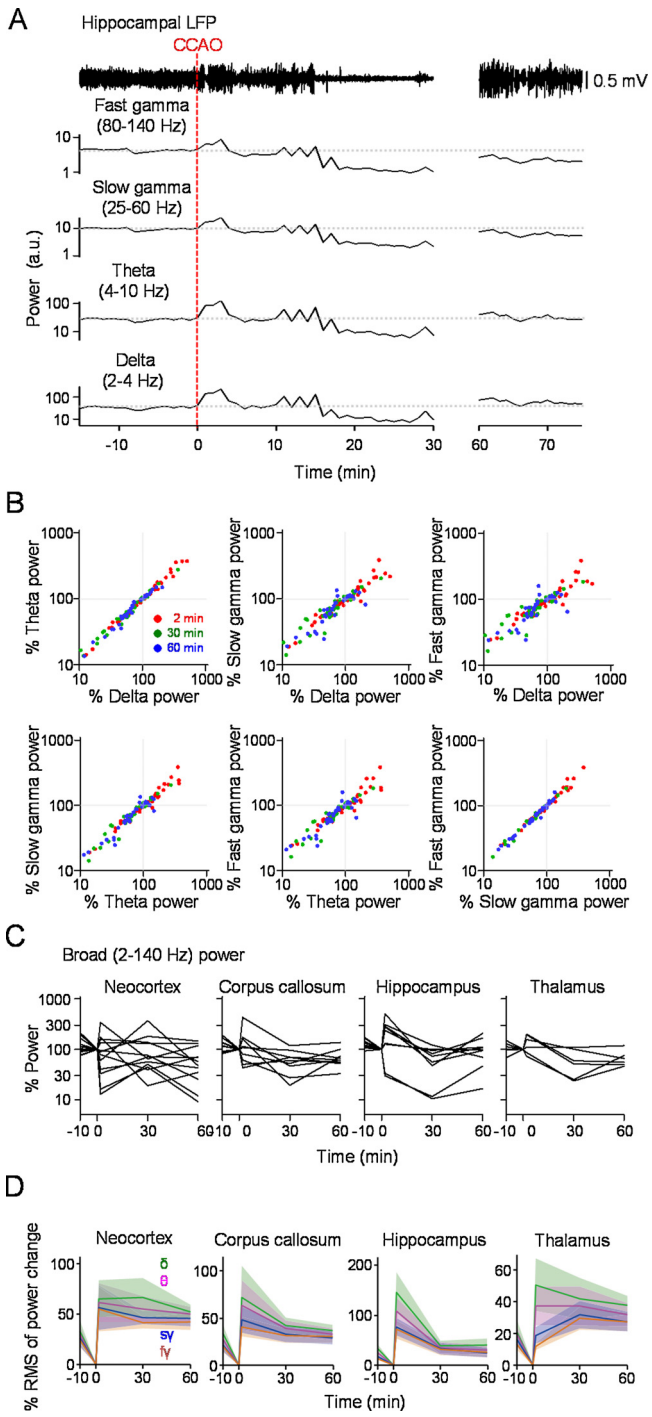

Fig. 2. Time course of the changes in LFP power following acute CCAO-induced hypoperfusion. (A) A representative LFP recording from the hippocampus (top) and the corresponding LFP power in the fast gamma, slow gamma, theta, and delta bands (bottom 4 panels). The gray lines represent baseline power during the pre-occlusion period. (B) Relationship of CCAO-induced LFP power changes between two frequency bands. For each electrode, the ratios of LFP power at 2 min, 30 min, and 1 h after CCAO to the power at 2 min before CCAO were plotted. All pairs had significant positive correlations. (C) Time changes in LFP power at a broad frequency (2–140 Hz) band after CCAO in individual brain regions. Each line represents a single recording electrode (neocortex, $n = 12$; corpus callosum, $n = 9$; hippocampus, $n = 9$; thalamus, $n = 6$). Data were normalized to the power at 0–2 min before CCAO at the individual recording sites. (D) Average percentage of the root mean square (RMS) of LFP power relative to the baseline values at 0 min, representing absolute changes in LFP power. Statistical significance is summarized in Table 1.

body weight, intraperitoneal injection). After restraining the mice on a custom-made stereotaxic apparatus (Narishige), the skull was exposed with an incision of the scalp and a craniotomy was performed using a high speed drill. The opening ($2.0 \times 2.0\,mm^2$) was centered at 1.4 mm posterior and 1.4 mm lateral to the bregma. An optical fiber (200 μm core diameter, 0.48 numerical aperture, Thorlabs) epoxied to ceramic zirconia ferrules (Precision Fiber Products) was unilaterally inserted into the brain, along with recording electrodes, in the center of the opening (Fig. 3A). After beginning the electrophysiological recordings, the photosensitive dye rose bengal (200 mg/kg, Waldeck GmbH & Co. KG) was administered intraperitoneally. To activate the dye, stimulation with green light (561 nm wavelength) was focally applied 10 min after the injection and maintained for 10–15 min. The intensity of the light at the tip of the plastic fiber was 2.3–4.9 mW.

2.3. Electrophysiological recording

For electrophysiological recording, the mice were anesthetized with urethane (1.0 g/kg, intraperitoneal injection) and restrained with their head held in place by a metal plate. A craniotomy was performed to create a hole ($2.0 \times 2.0\,mm^2$) centered at 1.4 mm posterior and 1.4 mm lateral to the bregma using a high-speed drill, and the dura was surgically removed. Two stainless-steel screws were implanted in the bone above the cerebellum to serve as ground and reference electrodes. A microdrive was used to hold an electrode assembly that consisted of 6–8 electrode wires, which was designed and created using a 3-D printer (UP Plus 2, Delta Micro Factory Corporation). Before inserting them into the brain, the length of individual tetrodes was adjusted so that the final depth in the brain ranged from 500 to 3500 μm. The assembly was inserted into the exposed area at a speed of 10 μm/s. The electrodes were allowed to stabilize at their final position for 30 min before recording began. The electrodes were constructed from 17-μm-wide polyimide-coated platinum-iridium (90/10%) wire (California Fine Wire), and the electrode tips were plated with platinum to lower electrode impedances to 150–300 kΩ at 1 kHz. To aid in the reconstruction of the tracks left by the electrodes, the electrodes were coated with DiI fluorophores that were applied by dipping the electrode tips into a DiI solution (80 mg/mL, Invitrogen) dissolved in 1:1 acetone/ethanol for 60 s before insertion. Electrophysiological data were sampled at 2 kHz using a Cereplex direct recording system (Blackrock). Recording began after stable neuronal unit activity was observed. At the end of the recording, the electrodes stained with DiI were carefully removed from the brain, unless otherwise specified. For CCAO experiments, occlusion of the left common carotid artery was confirmed, and only the animals with successful CCAO were included in the data analysis. Recordings were performed at a room temperature of 22–25 °C.

2.4. Histological analysis to confirm electrode and optical fiber locations

For 16 mice, electrodes and optical fibers were stained with DiI as described above before insertion into the brain. The mice were perfused intracardially with cold 4% paraformaldehyde (PFA) in 25 mM phosphate-buffered saline (PBS) and decapitated. The brains were coronally sectioned at a thickness of 100 μm. For 1 mouse, the electrodes were not stained with DiI, and they were left in place after the final recording session. This mouse was then intracardially perfused with cold 4% PFA in 25 mM PBS and decapitated. To aid the reconstruction of the electrode tracks, the electrodes were not withdrawn from the brain of this mouse until 12 h after perfusion. After dissection, the brains were fixed overnight in 4% PFA and then equilibrated with a sequence of 20% sucrose and 30% sucrose in phosphate-buffered saline.

Frozen coronal sections (40 μm) were obtained, and serial sections were rinsed in water, counterstained with cresyl violet, and coverslipped with Permount. Recordings were included in the data analysis only if the electrode's deepest position was in the targeted brain regions.

2.5. TTC staining

For 2,3,5-triphenyltetrazolium chloride (TTC) staining, the animals were sacrificed and the brains were removed 12 h after hippocampal ischemia induction and coronal brain slices with a thickness of 400 μm were obtained with a vibratome (Dosaka EM). Slices were immediately immersed in 2% TTC in artificial CSF at 37 °C for 30 min.

2.6. Data analysis

The power spectra of 2-min LFP signals were calculated by fast Fourier transformation using Matlab. The power of LFPs in the following sub-frequency bands was calculated: delta (2–4 Hz), theta (4–10 Hz), slow gamma (25–60 Hz), and fast gamma (80–140 Hz). In acute CCAO experiments, baseline power for statistical comparisons was defined as LFP power 0–2 min before application of CCAO. The ratio of SD (standard deviation) to mean (i.e. coefficient of variation) of LFP power during a pre-CCAO period was 21.8%. Based on this value, we defined the threshold to detect significance as a 50% (1.5 fold) change, which corresponds with $\alpha = 0.02$. All values are reported as the mean ± SEM. To identify significant differences, we performed Tukey's test after one-way analysis of variance (ANOVA), Dunnett's test after repeated measures ANOVA, or a Mann–Whitney *U* test.

3. Results

3.1. Regional differences in neuronal network dynamics with acute hypoperfusion

To induce a global hypoxic/ischemic condition in the forebrain while performing in vivo electrophysiological recordings, we used unilateral common carotid artery occlusion (CCAO) (Ohtaki et al., 2005), a technique that reduces the blood supply to the forebrain (Fig. 1A). Local field potential (LFP) signals were recorded from the deep layers of the neocortex, the corpus callosum, the dorsal hippocampus, and the thalamus of urethane-anesthetized mice. The tracks of electrodes stained with DiI were identified histologically in the tissue (Fig. 1B). After obtaining 20 min of stable recordings, CCAO was rapidly induced and the LFP signals were continuously monitored for up to 80 min (Fig. 1C). These recordings were obtained from 7 mice. To validate that no pronounced LFP changes occur without CCAO, we performed additional experiments from a sham-operated mouse group in which the left common carotid artery was exposed and a loop of an elastic string was formed around the artery, same as in CCAO, but the artery was not closed (Fig. 1D). In this group, no significant time-dependent changes in LFP power were observed for up to 80 min (neocortex, $n = 6$ channels from 4 mice, $F = 0.78$, $P = 0.59$; hippocampus/corpus callosum, $n = 12$ channels from 4 mice, $F = 1.72$, $P = 0.13$; repeated measures ANOVA).

Cortical LFP patterns were classified by type into delta (2–4 Hz), theta (4–10 Hz), slow gamma (25–60 Hz), and fast gamma (80–140 Hz) oscillations. As shown in a representative example in Fig. 2A, a transient change in LFP power was observed after CCAO. Although the degree and direction of power changes varied across recording sites, the temporal changes in LFP power at different oscillatory bands within a recording site appeared to be correlated with each other. To quantify this property, we plotted the ratio of LFP power after CCAO to that before CCAO for pairs of oscillatory bands (Fig. 2B). The plots revealed significant positive correlations in all pairs of LFP bands (delta vs. theta, $R = 0.98$, $P = 2.8 \times 10^{-79}$; delta vs. slow gamma, $R = 0.88$, $P = 7.5 \times 10^{-37}$; delta vs. fast gamma, $R = 0.82$, $P = 3.7 \times 10^{-27}$; theta vs. slow gamma, $R = 0.95$, $P = 8.7 \times 10^{-54}$; theta vs. fast gamma, $R = 0.89$, $P = 3.6 \times 10^{-37}$; slow gamma vs. fast gamma, $R = 0.99$, $P = 1.6 \times 10^{-82}$, Spearman's test), demonstrating that LFP changes in response to CCAO showed a similar tendencies across different oscillatory bands within the same recording site.

Although the changes in the patterns of LFP power were heterogeneous within each brain area, the recordings at most sites started to show a prominent change in power as early as 2 min after CCAO (Fig. 2C), indicating that a disruption of the functions of the cortical network occurred a few minutes after CCAO-induced hypoperfusion. In the neocortex, the corpus callosum, the dorsal hippocampus, and the thalamus, 66.7%, 77.8%, 77.8%, 50% of electrodes showed a 1.5-fold increase or decrease in the 2–140 Hz LFP power 2 min after CCAO, compared with the pre-occlusion period, respectively. To quantify how the disruption in network activity after CCAO behaved over time, we calculated the root mean square (RMS) of LFP power, which represents the absolute rates of changes in LFP power relative to the baseline values (Fig. 2D). A summary of the significant changes in LFP power between pre-occlusion and post-occlusion periods are summarized in Table 1. In the neocortex, there were significant changes in absolute power at the delta and theta bands at all time points during the recording session (Table 1). In addition, 50% and 58.3% of electrodes showed a 1.5-fold decrease in the 2–140 Hz LFP power 30 and 60 min, respectively, after CCAO. These results suggest that network activity levels in the neocortex continuously decreased during hypoperfusion. In the corpus callosum and the hippocampus, the average absolute rates of change were less pronounced over time, and no significant differences were observed at 30 min after CCAO, with the exception of fast gamma power in the corpus callosum (Table 1). These results demonstrate that these two brain regions are able to recover their network activity levels during periods of reduced perfusion. In the thalamus, absolute power changes in lower frequency bands (i.e., delta and theta bands) became less prominent with time, whereas those in higher frequency bands (i.e., slow gamma and fast gamma

Table 1
Summary of the significance of LFP power changes shown in Fig.2D. LFP power at individual frequency bands was compared between pre-CCAO and post-CCAO periods at 2 min, 30 min, and 60 min after the induction of CCAO. *P* values less than 0.05 are considered statistically significant (Tukey's test).

	2 min	30 min	60 min
Neocortex			
Delta	$P^* = 7.2 \times 10^{-3}$	$P^* = 5.9 \times 10^{-3}$	$P^* = 0.043$
Theta	$P^* = 3.5 \times 10^{-3}$	$P^* = 7.2 \times 10^{-3}$	$P^* = 0.022$
Slow gamma	$P^* = 0.010$	$P^* = 0.046$	$P = 0.052$
Fast gamma	$P^* = 0.012$	$P = 0.083$	$P = 0.072$
Corpus callosum			
Delta	$P^* = 0.027$	$P = 0.33$	$P = 0.44$
Theta	$P^* = 0.016$	$P = 0.22$	$P = 0.37$
Slow gamma	$P^* = 2.8 \times 10^{-3}$	$P = 0.057$	$P = 0.12$
Fast gamma	$P^* = 1.9 \times 10^{-3}$	$P^* = 0.021$	$P^* = 0.026$
Hippocampus			
Delta	$P^* = 2.3 \times 10^{-4}$	$P = 0.60$	$P = 0.55$
Theta	$P^* = 1.4 \times 10^{-4}$	$P = 0.41$	$P = 0.50$
Slow gamma	$P^* = 2.9 \times 10^{-4}$	$P = 0.20$	$P = 0.43$
Fast gamma	$P^* = 8.5 \times 10^{-4}$	$P = 0.24$	$P = 0.42$
Thalamus			
Delta	$P^* = 0.018$	$P = 0.060$	$P = 0.10$
Theta	$P^* = 0.049$	$P = 0.050$	$P = 0.11$
Slow gamma	$P = 0.14$	$P^* = 5.1 \times 10^{-3}$	$P^* = 0.017$
Fast gamma	$P = 0.33$	$P^* = 1.5 \times 10^{-3}$	$P^* = 3.3 \times 10^{-3}$

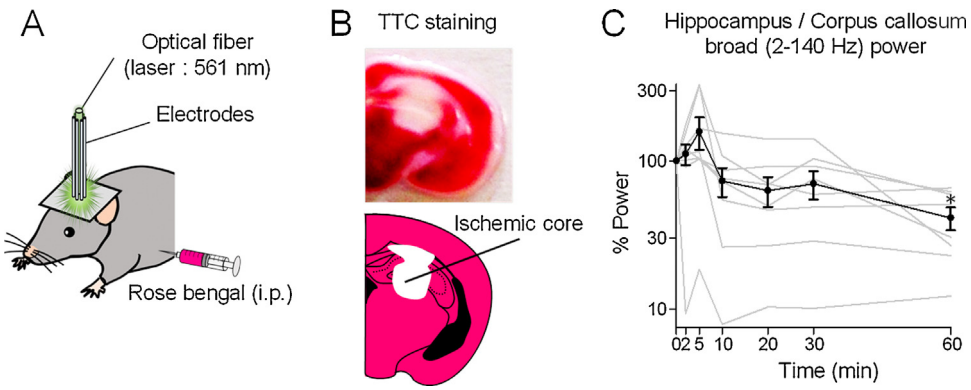

Fig. 3. Time changes in LFP power following acute photothrombosis. (A) Illustration of the procedure. Rose bengal was injected intraperitoneally and focal ischemia was induced by applying photostimulation to the dye via an optic fiber in the corpus callosum and the hippocampus. (B) Representative TTC staining showing the creation of a focal ischemic core after photothrombosis. (C) Time changes in LFP power at a broad frequency (2–140 Hz) band after photothrombosis in individual brain regions ($n = 8$ recordings from 3 mice). Each line represents a single recording electrode. Data were normalized to the power at 0 min at the individual recording sites. Repeated measures ANOVA revealed a significant time-dependent change in LFP power ($F(6,42) = 5.74$; $P = 0.0002$). $^{*}P < 0.05$, Dunnett's test.

bands) became significant at 30 min after CCAO (Table 1). These results suggest that adaptability to hypoxic conditions in the thalamus varies depending on the oscillatory patterns observed.

3.2. Focal photothrombosis triggers irreversible power reduction in the corpus callosum and hippocampus

CCAO-induced hypoperfusion was not sufficient to elicit long-lasting neuronal activity changes in the hippocampus. To test how more severe ischemic damage alters network activity in the hippocampus, we next tested the effect of photothrombosis, a model of ischemia that significantly reduces blood supply, to induce neuronal degeneration in a small area of the brain (Labat-gest and Tomasi, 2013). In this model, the formation of a clot in brain blood vessels was produced by applying photostimulation to the photosensitive dye rose bengal injected into the circular system (Watson et al., 1985). An optical fiber with a diameter of 200 μm was inserted above the recording sites of the corpus callosum and the hippocampus (Fig. 3A). After obtaining 30 min of stable recordings, rose bengal was intraperitoneally injected, and the site was stimulated 10 min later for 10–15 min with green light (561 nm). A focal ischemic core in the illuminated area was verified by TTC staining (Fig. 3B). Similar to CCAO, hippocampal activity showed an immediate change in response to photothrombosis (Fig. 3C). After a transient elevation of LFP power, which occurred within a few minutes of stimulation, the percentages of 2–140 Hz LFP power continuously decreased to 73.3 ± 16.2%, 70.1 ± 15.0%, and 41.3 ± 7.2% at 10 min, 30 min, and 60 min, respectively, after the onset of photostimulation. These results suggest that LFP power within the hippocampus never returned to the pre-photostimulation baseline when significant ischemia related to neuronal degeneration was induced.

3.3. Changes in neuronal activity after a chronic hypoxic state

We next examined long-lasting changes in the neuronal activity patterns in mice under chronic CCAO-induced forebrain hypoperfusion (chronic CCAO mice). After the CCAO surgery, animals were continuously subject to CCAO for 7 days. During the post-surgery period, all 9 mice survived. On day 7 after surgery, the mice were anesthetized with urethane for extracellular recordings using the same methods as in the acute CCAO experiments. Two of the 9 mice died under anesthesia, probability due to the effects of forebrain hypoperfusion. The remaining 7 animals were used for the chronic CCAO experiment. For comparison, the data obtained from the mice before application of CCAO in Fig. 2 were defined as data from control mice. Recording sites in these animals are shown in Fig. 4A. In the neocortex of chronic CCAO mice, LFP power at all frequency bands was 1.3–2.5 times lower than that in the control mice that did not undergo CCAO (Fig. 4B). Only the delta band, the lowest frequency band, showed a significant decrease in power (delta, $U = 19$, $P = 0.028$; theta, $U = 27$, $P = 0.11$; slow gamma, $U = 35$, $P = 0.34$; fast gamma, $U = 40$, $P = 0.56$). In the hippocampus, we found pronounced increases in the power of the theta, slow gamma, and fast gamma bands of chronic CCAO mice (delta, $U = 37$, $P = 0.074$; theta, $U = 23$, $P = 0.009$; slow gamma, $U = 20$, $P = 0.005$; fast gamma, $U = 24$, $P = 0.01$). No significant differences in LFP power were observed between control and chronic CCAO mice in the corpus callosum and the thalamus (corpus callosum: delta, $U = 26$, $P = 0.95$; theta, $U = 22$, $P = 0.60$; slow gamma, $U = 15$, $P = 0.18$; fast gamma, $U = 13$, $P = 0.11$; thalamus: delta, $U = 12$, $P = 1.00$; theta, $U = 9$, $P = 0.61$; slow gamma, $U = 11$, $P = 0.91$; fast gamma, $U = 10$, $P = 0.76$), suggesting that activity patterns in these brain regions returned to normal during the 7 days of chronic hypoxia.

4. Discussion

Using a multi-channel extracellular recording technique, we examined how cerebral hypoperfusion alters neuronal activity patterns in the thalamo-cortico-hippocampal network. The main findings of our study are as follows: (1) these brain regions showed heterogeneous changes in their LFP power in response to CCAO-induced hypoperfusion, (2) the hippocampus and the corpus callosum, but not the neocortex, were able to restore neurophysiological activity against CCAO-induced hypoperfusion by reducing the fluctuations in the LFP power changes, and (3) LFP power was potentiated and depressed in the hippocampus and the neocortex, respectively, in mice chronically exposed to 7-day of CCAO-induced hypoperfusion. The chronic depression of the LFP power in the neocortex might be related to the inability to regain normal LFP patterns during acute CCAO-induced hypoperfusion. However, the chronic potentiation of hippocampal LFP power might be due to excessive rebound of neuronal activity, a mechanism that might be partly related to the acute (<30 min) recovery effect in response to the hypoperfusion. The sensitivity of neuronal activity patterns to hypoperfusion may thus serve as a neurophysiological sign of the subsequent chronic dysfunction of neuronal networks.

To mimic ischemic stroke, in vivo mouse models have been established for use in cerebrovascular research. These models include middle cerebral artery occlusion (MCAO), CCAO, and photothrombosis (Barth and Mody, 2011; Durukan and Tatlisumak,

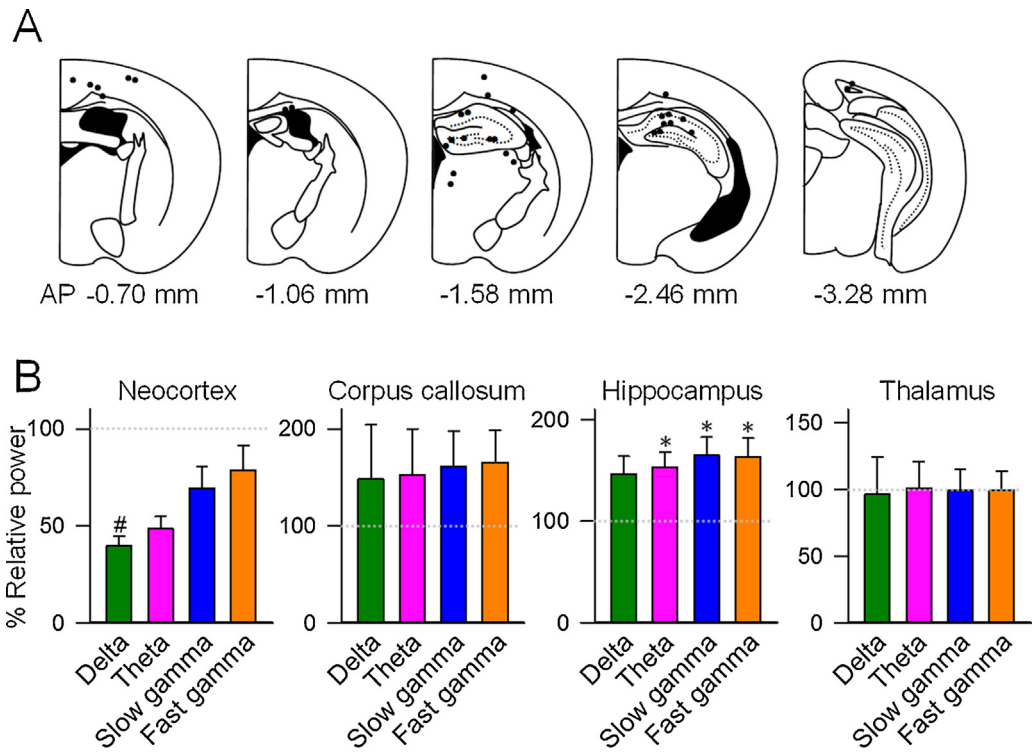

Fig. 4. Changes in neuronal network activity after chronic CCAO-induced hypoperfusion. (A) Histological verification of recording sites in sequential coronal brain sections of chronic CCAO mice. Black dots indicate the endpoints of the electrode tracts ($n = 7$ mice). (B) The percentage of LFP power in chronic CCAO mice normalized to average power in control mice without hypoperfusion. * and # indicate a significant increase and decrease, respectively, between control and chronic CCAO mice. $P < 0.05$, Mann–Whitney U test.

2007). MCAO and photothrombosis focally induce brain ischemia by significantly reducing blood flow. We confirmed that photothrombosis causes an irreversible disruption of LFP signals in the ischemic core of the hippocampus, which is associated with the progression of neuronal cell death (Labat-gest and Tomasi, 2013). Unlike the focal ischemia models, the unilateral CCAO used in this study induces a global hypoxic state by reducing the circulatory flow rate in the forebrain without inducing severe neuronal loss. In this model, we demonstrated that some brain regions were able to return to their normal activity levels within 1 h and that these activity levels lasted for up to a week. We note that our data was obtained from urethane-anesthetized mice. It has been shown that treatment of urethane affects several types of ongoing oscillations such as theta and slow wave oscillations in the cortex. Further studies are needed to clarify our finding is applicable to awake, drug-free animals.

Several mechanisms may account for the greater ability to resist change in response to CCAO-induced hypoperfusion in the thalamus and the hippocampus. First, these brain regions might be more efficiently covered by a compensatory redistribution of blood flow from the circulatory system via the circle of Wills. Second, inherent recurrent connections between neurons or the rapid reorganization of functional connections may allow these regions to retain their normal network activity patterns under conditions of decreased perfusion. In addition, it has been widely demonstrated that a variety of cellular and molecular mechanisms are mobilized during hypoxic/ischemic states, such as intracellular acidosis (Vannucci and Yager, 1992), glutamate release (Benveniste et al., 1989; Nishizawa, 2001), ATP production (Lifshitz et al., 2003), and the activation/deactivation of signaling pathways associated with neuronal cell death (Durukan and Tatlisumak, 2007; Eltzschig and Eckle, 2011; Wei et al., 2004). It remains unknown how these mechanisms might account for regional differences in the vulnerability to the hypoperfusion.

In neurophysiological studies, the application of unilateral CCAO is considered a model for perturbing neuronal activity within a few minutes. Our findings demonstrate that neuronal populations in specific brain regions form a rigid homeostatic system to maintain the overall power of organized oscillatory activity in the presence of an intense external perturbation. As a pathophysiological study, our findings of regional differences may help explain hypoperfusion-associated symptoms observed in both animals and humans and may help in developing therapeutic strategies to reduce or reverse brain dysfunction due to hypoxic/ischemic damage.

Conflict of interest

The authors declare that there are no conflicts of interest.

Acknowledgments

This work was supported by Kaken-hi (15H05569 and 15H01417), the Takeda Science Foundation, the Research Foundation for Pharmaceutical Sciences, and the Kobayashi International Scholarship Foundation.

References

Barth, A.M., Mody, I., 2011. Changes in hippocampal neuronal activity during and after unilateral selective hippocampal ischemia in vivo. J. Neurosci. 31, 851–860.
Benveniste, H., Jorgensen, M.B., Sandberg, M., Christensen, T., Hagberg, H., Diemer, N.H., 1989. Ischemic damage in hippocampal CA1 is dependent on glutamate release and intact innervation from CA3. J. Cereb. Blood Flow Metab. 9, 629–639.
Buzsaki, G., 2006. Rhythms of the Brain. Oxford University Press, New York.
Buzsaki, G., Freund, T.F., Bayardo, F., Somogyi, P., 1989. Ischemia-induced changes in the electrical activity of the hippocampus. Exp. Brain Res. 78, 268–278.
Durukan, A., Tatlisumak, T., 2007. Acute ischemic stroke: overview of major experimental rodent models, pathophysiology, and therapy of focal cerebral ischemia. Pharmacol. Biochem. Behav. 87, 179–197.

Eltzschig, H.K., Eckle, T., 2011. Ischemia and reperfusion—from mechanism to translation. Nat. Med. 17, 1391–1401.
Labat-gest, V., Tomasi, S., 2013. Photothrombotic ischemia: a minimally invasive and reproducible photochemical cortical lesion model for mouse stroke studies. J. Vis. Exp.
Lifshitz, J., Friberg, H., Neumar, R.W., Raghupathi, R., Welsh, F.A., Janmey, P., Saatman, K.E., Wieloch, T., Grady, M.S., McIntosh, T.K., 2003. Structural and functional damage sustained by mitochondria after traumatic brain injury in the rat: evidence for differentially sensitive populations in the cortex and hippocampus. J. Cereb. Blood Flow Metab. 23, 219–231.
Monmaur, P., Thomson, M.A., M'Harzi, M., 1986. Temporal changes in hippocampal theta activity following twenty minutes of forebrain ischemia in the chronic rat. Brain Res. 378, 262–273.
Nishizawa, Y., 2001. Glutamate release and neuronal damage in ischemia. Life Sci. 69, 369–381.
Ohtaki, H., Dohi, K., Nakamachi, T., Yofu, S., Endo, S., Kudo, Y., Shioda, S., 2005. Evaluation of brain ischemia in mice. Acta Histochem. Cytochem. 38, 99–106.
Vannucci, R.C., Yager, J.Y., 1992. Glucose, lactic acid, and perinatal hypoxic-ischemic brain damage. Pediatr. Neurol. 8, 3–12.
Watson, B.D., Dietrich, W.D., Busto, R., Wachtel, M.S., Ginsberg, M.D., 1985. Induction of reproducible brain infarction by photochemically initiated thrombosis. Ann. Neurol. 17, 497–504.
Wei, L., Ying, D.J., Cui, L., Langsdorf, J., Yu, S.P., 2004. Necrosis, apoptosis and hybrid death in the cortex and thalamus after barrel cortex ischemia in rats. Brain Res. 1022, 54–61.